atmosphere

MDPI

Supplementary Materials:

Convection-Permitting Future Climate Simulations for Bulgaria under the RCP8.5 Scenario

Rilka Valcheva *, Ivan Popov and Nikola Gerganov

National Institute of Meteorology and Hydrology, 1784 Sofia, Bulgaria; ivan.popov@meteo.bg (I.P.); nikola.gerganov@meteo.bg (N.G.)

* Correspondence: rilka.valcheva@meteo.bg

This document provides Figures (from S1 to S10) representing the daily scale analysis not shown in the main text. Figures S1 to S6 are dedicated to the assessment of the historical period 1995–2004, representing means and biases for the seasonal mean daily precipitation, wet-day intensity, frequency, and heavy precipitation (p99) for all seasons. Figure S7 shows the probability density function (PDF) of the daily precipitation for Bulgaria from simulations and observations Figures S8 to S10 report the changes over the end of the century 2089–2098 with respect to the historical period 1995–2004.

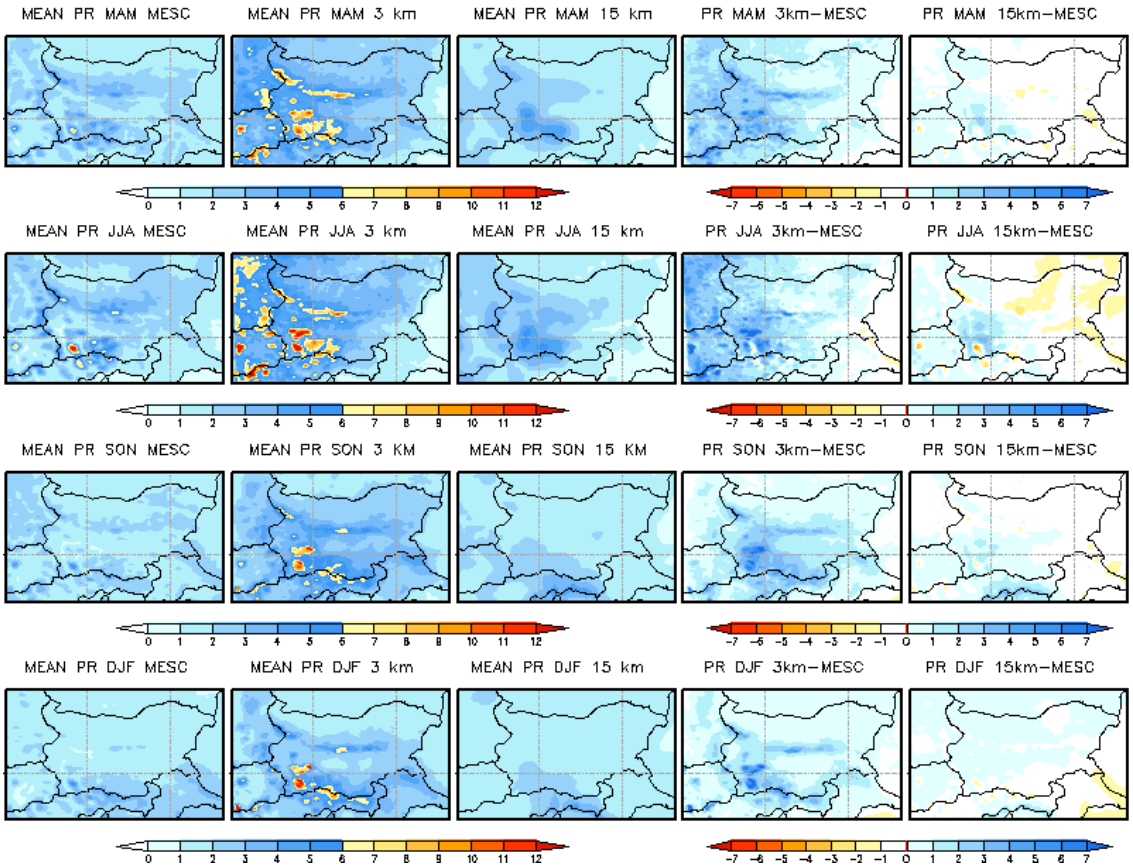

Figure S1. Spatial distribution of seasonal mean daily precipitation (mm/d) from observations (MESCAN-SURFEX) and simulations (3 km CPRCM and 15 km RCM) (first three columns) and mean biases of CPRCM and RCM with respect to MESCAN-SURFEX (last two columns) for the spring—MAM (first row), summer—JJA (second row), autumn—SON (third row) and winter—DJF (last row). The simulated historical period is 1995–2004.

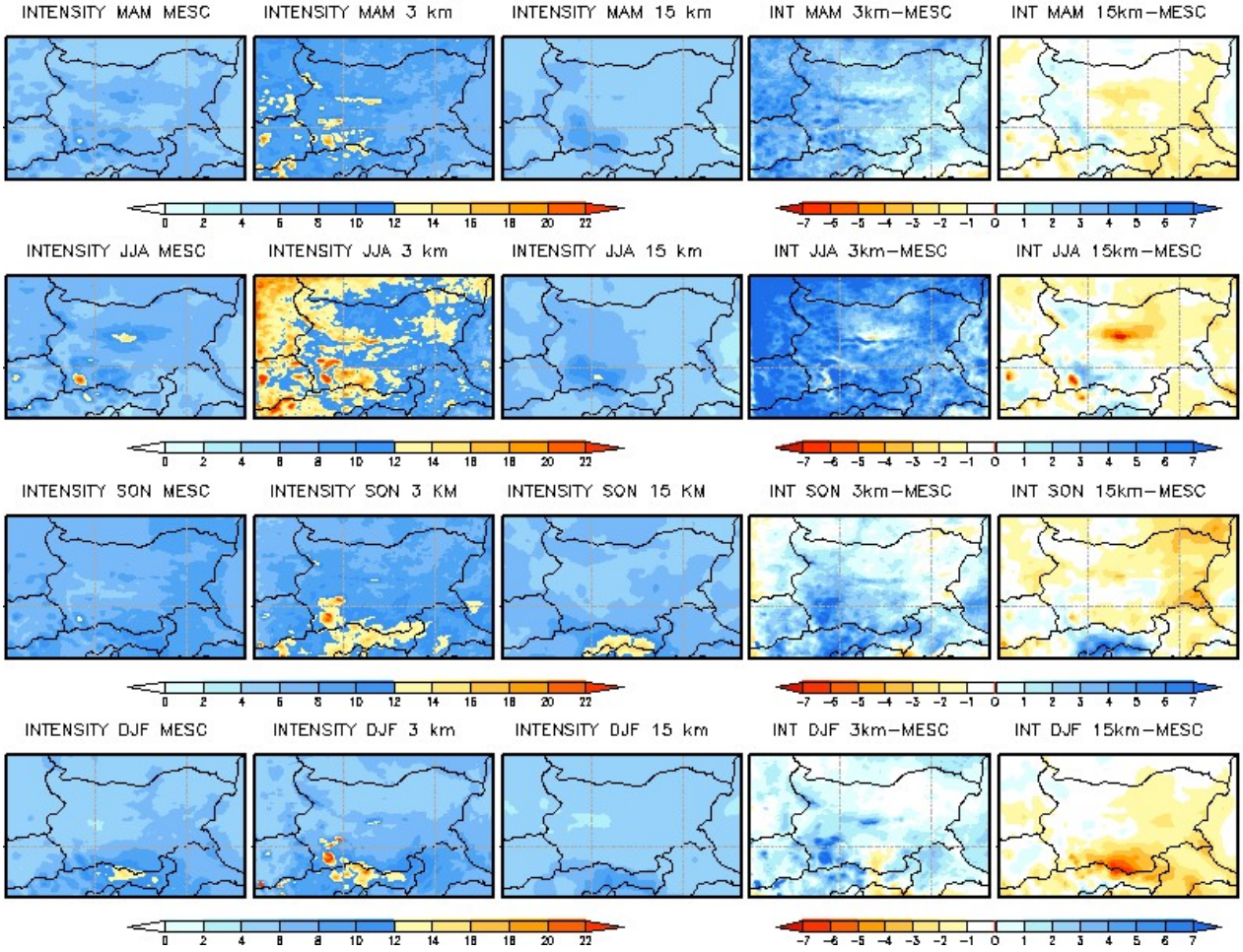

Figure S2. Spatial distribution of seasonal mean wet-day intensity (> 1 mm/d) in mm/d from observations (MESCAN-SURFEX) and simulations (3 km CPRCM and 15 km RCM) (first three columns) and mean biases of CPRCM and RCM with respect to MESCAN-SURFEX (last two columns) for the spring—MAM (first row), summer—JJA (second row), autumn—SON (third row) and winter—DJF (last row). The simulated historical period is 1995–2004.

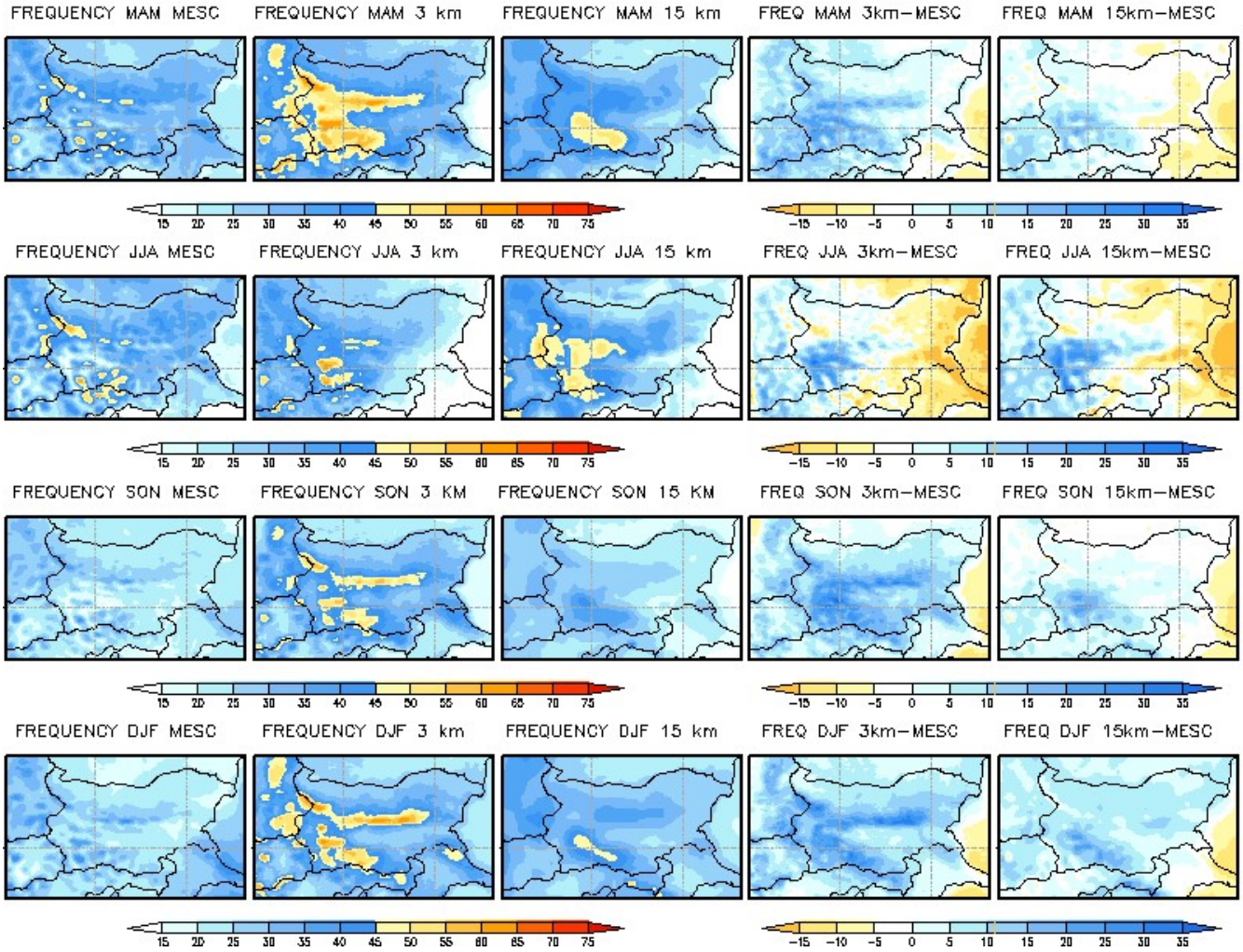

Figure S3. Spatial distribution of wet-day frequency (> 1 mm/d) in % from observations (MESCAN-SURFEX) and simulations (3 km CPRCM and 15 km RCM) (first three columns) and mean biases of CPRCM and RCM with respect to MESCAN-SURFEX (last two columns) for the spring—MAM (first row), summer—JJA (second row), autumn—SON (third row) and winter—DJF (last row). The simulated historical period is 1995–2004.

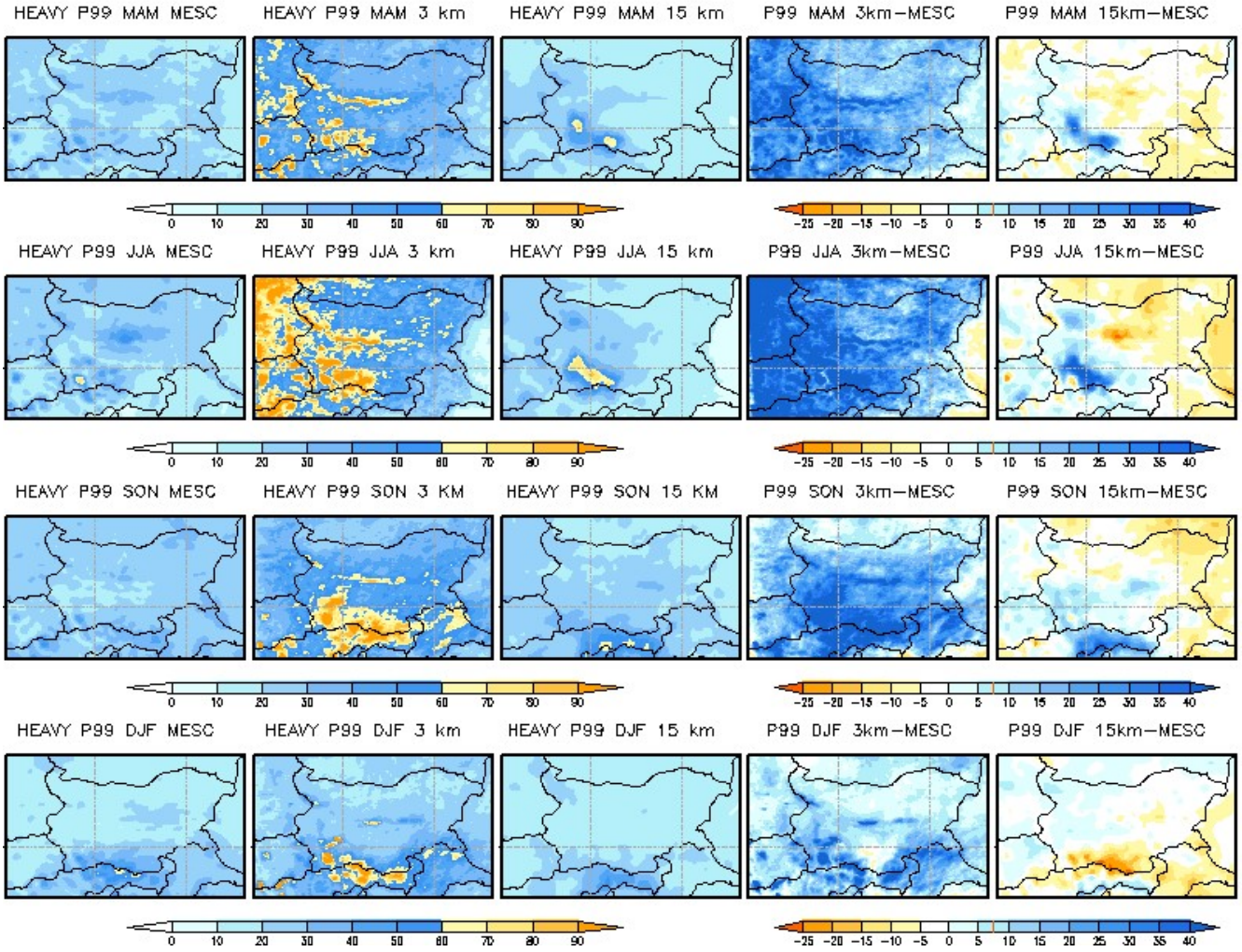

Figure S4. Spatial distribution of heavy precipitation (p99) in mm/d from observations (MESCAN-SURFEX) and simulations (3 km CPRCM and 15 km RCM) (first three columns) and mean biases of CPRCM and RCM with respect to MESCAN-SURFEX (last two columns) for the spring—MAM (first row), summer—JJA (second row), autumn—SON (third row) and winter—DJF (last row). The simulated historical period is 1995–2004.

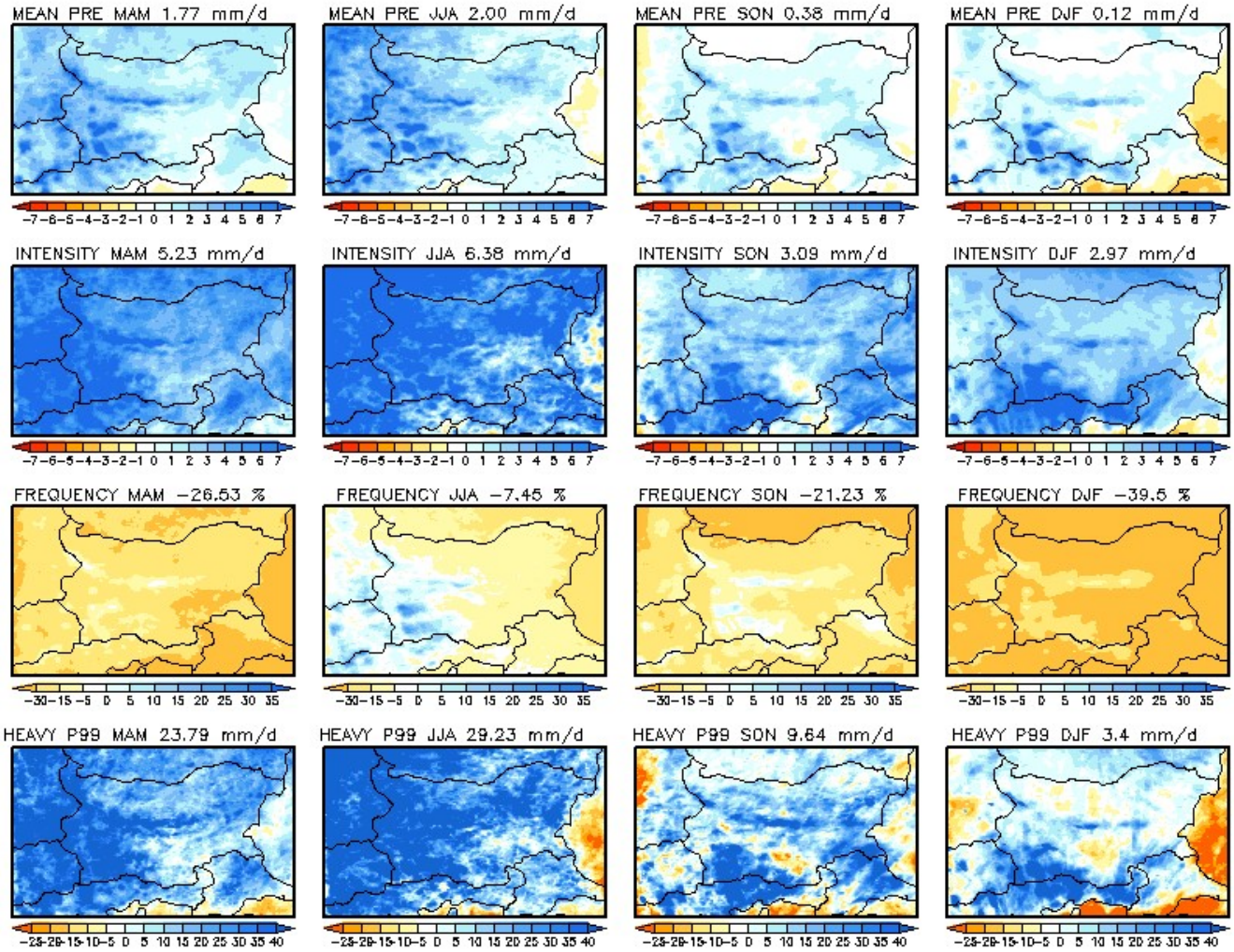

Figure S5. Spatial distribution of seasonal mean biases in the CPRCM simulation (3 km) with respect to the daily PDIR-Now dataset for mean daily precipitation in mm/d (first row), precipitation intensity (mm/d) (second row), frequency (%), and heavy precipitation (p99) in mm/d (last row) for the spring—MAM, summer—JJA, autumn—SON, and winter—DJF. The simulated historical period is 2001–2004. The area-average biases are on the top of each image.

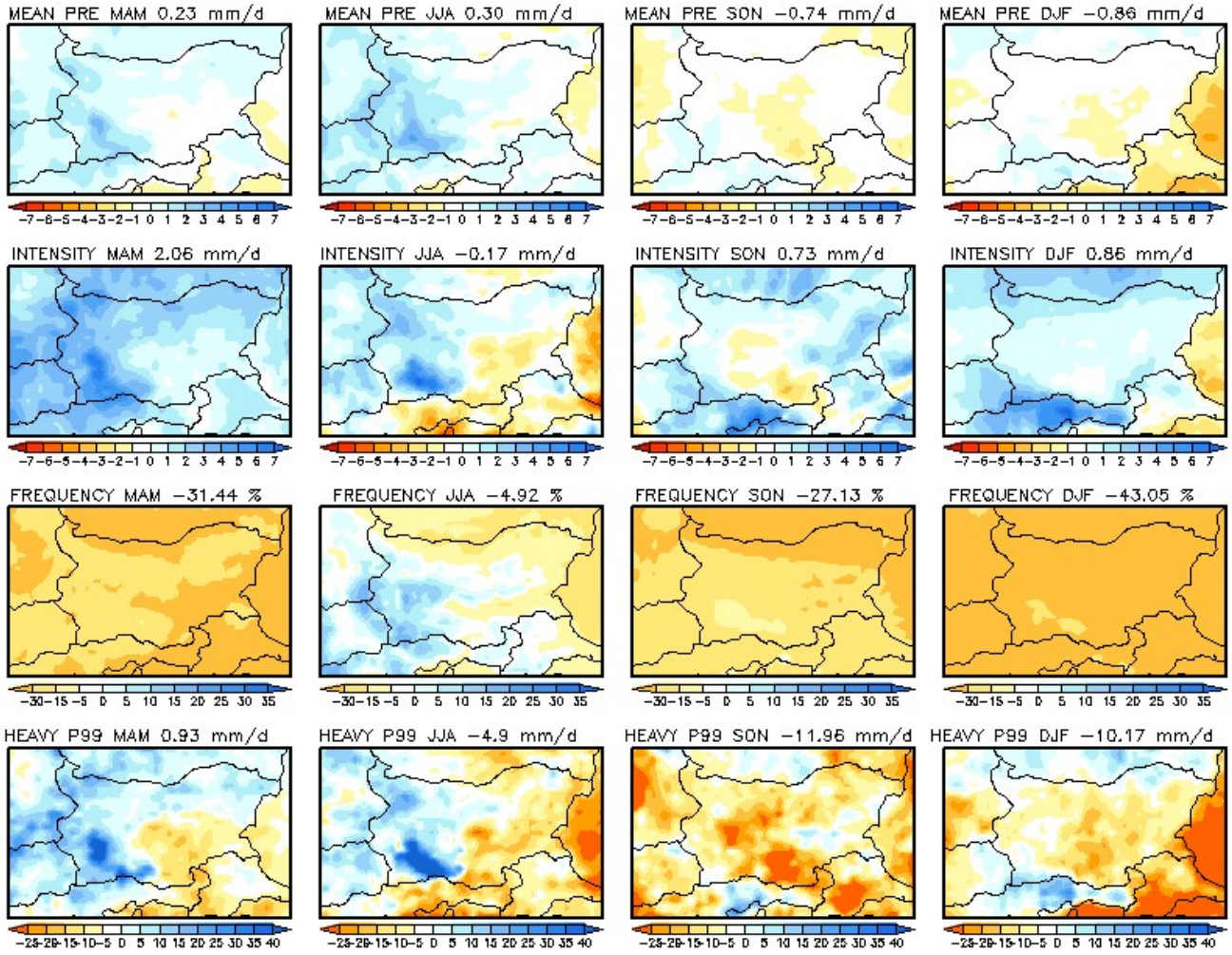

Figure S6. Spatial distribution of seasonal mean biases in the RCM simulation (15 km) with respect to the daily PDIR-Now dataset for mean daily precipitation in mm/d (first row), precipitation intensity (mm/d) (second row), frequency (%), and heavy precipitation (p99) in mm/d (last row) for the spring—MAM, summer—JJA, autumn—SON, and winter—DJF. The simulated historical period is 2001–2004. The area-average biases are on the top of each image.

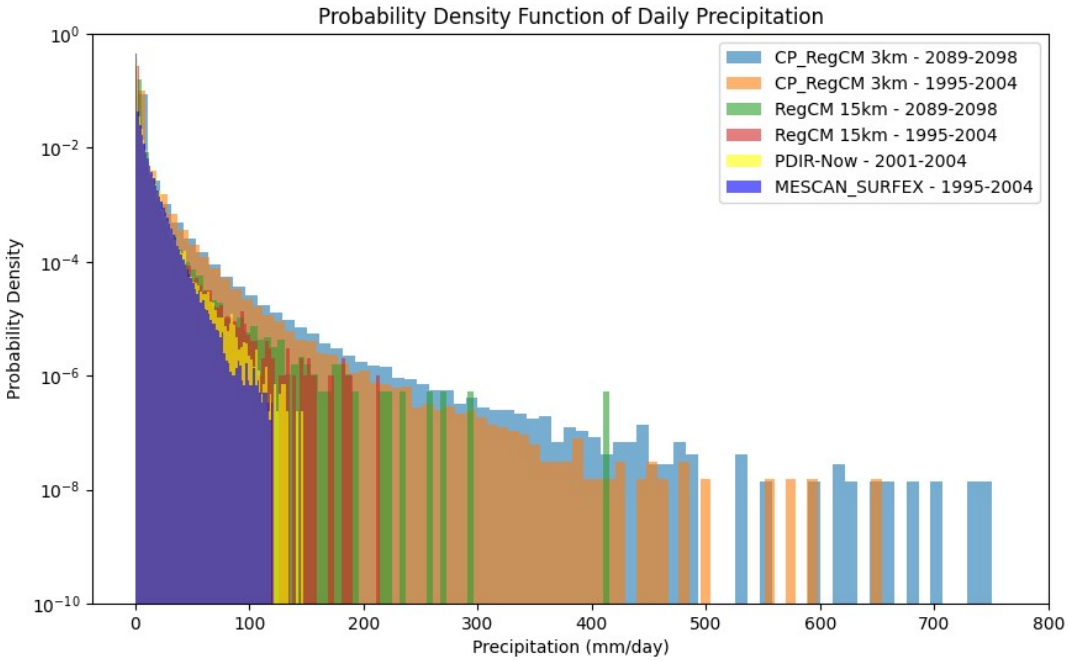

Figure S7. Probability density function (PDF) for the daily precipitation in Bulgaria from simulations (CPRCM and RCM) and observations (PDIR-Now and MESCAN-SURFEX) for the historical (1995–2004) and future periods (2089–2098). PDIR-Now is available for the period 2001–2004.

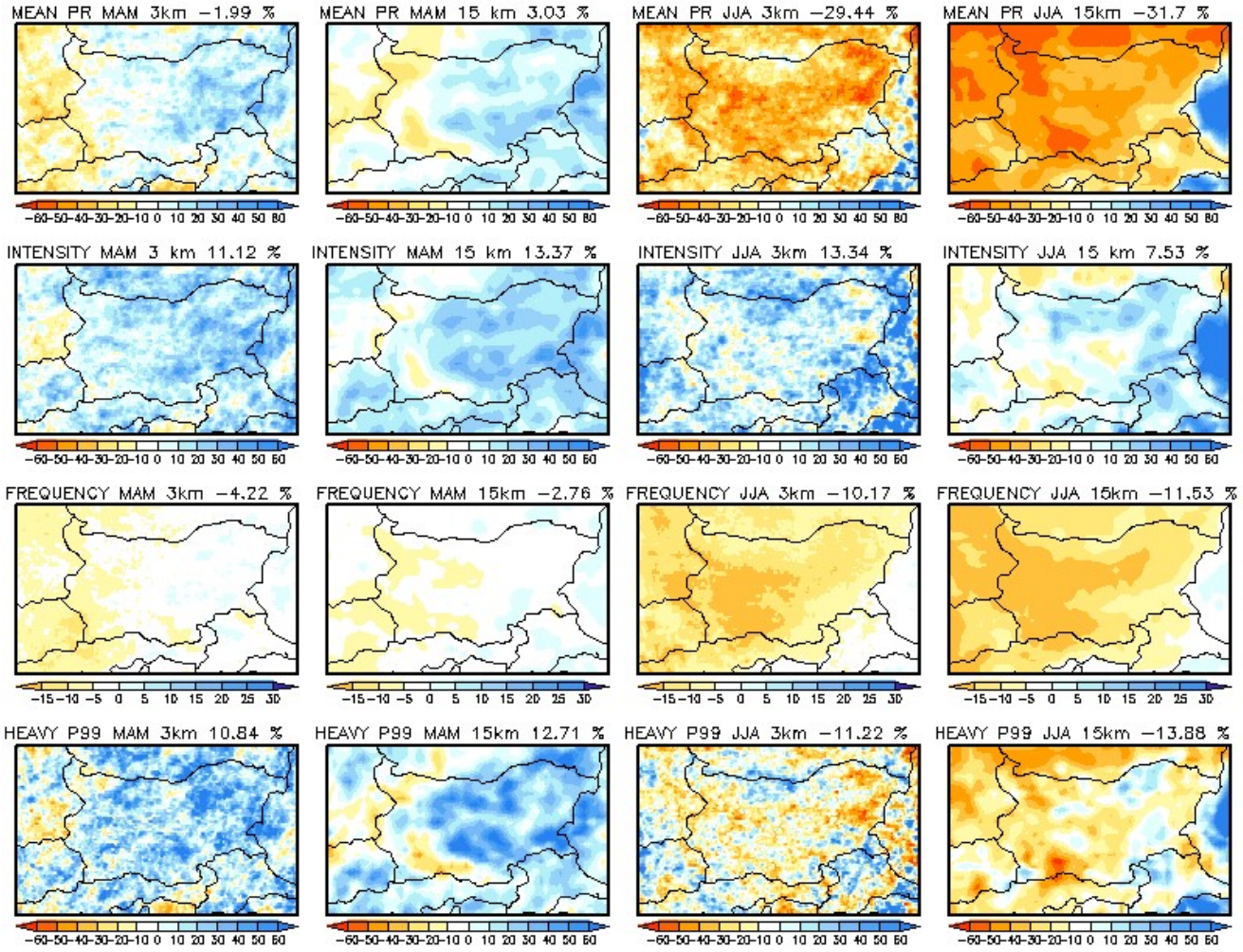

Figure S8. Expected changes in daily precipitation (first row), intensity (second row), frequency (third row), and heavy precipitation (p99) (last row) from both models (3 km CPRCM and 15km RCM) related to the spring—MAM (first two columns, respectively) and summer—JJA (last two columns, respectively) projected at the end of the century (2089–2098) with respect to the historical period (1995–2004) in %.

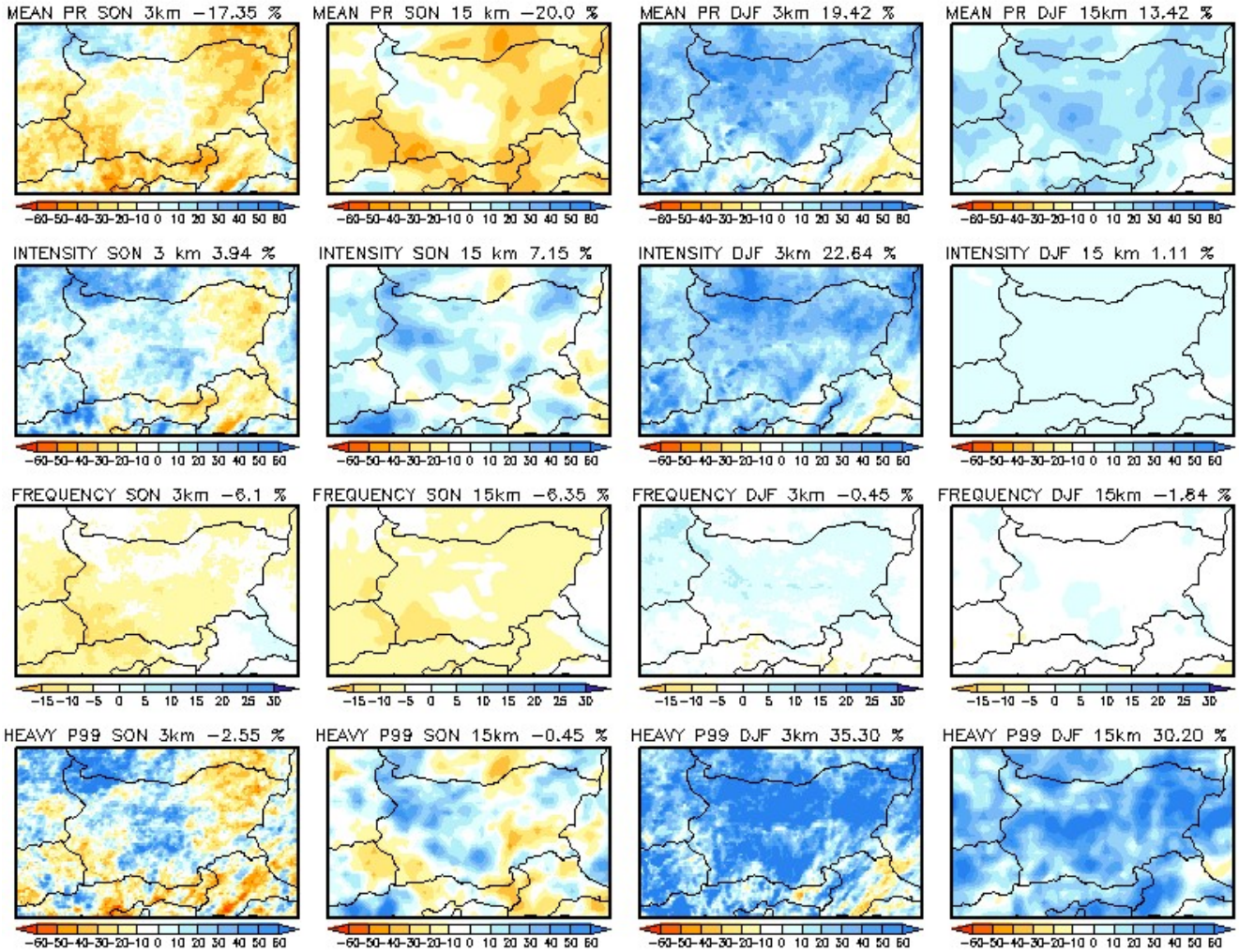

Figure S9. Expected changes in daily precipitation (first row), intensity (second row), frequency (third row), and heavy precipitation (p99) (last row) from both models (3 km CPRCM and 15km RCM) related to the fall—SON (first two columns, respectively) and winter—DJF (last two columns, respectively) projected at the end of the century (2089–2098) with respect to the historical period (1995–2004) in %.

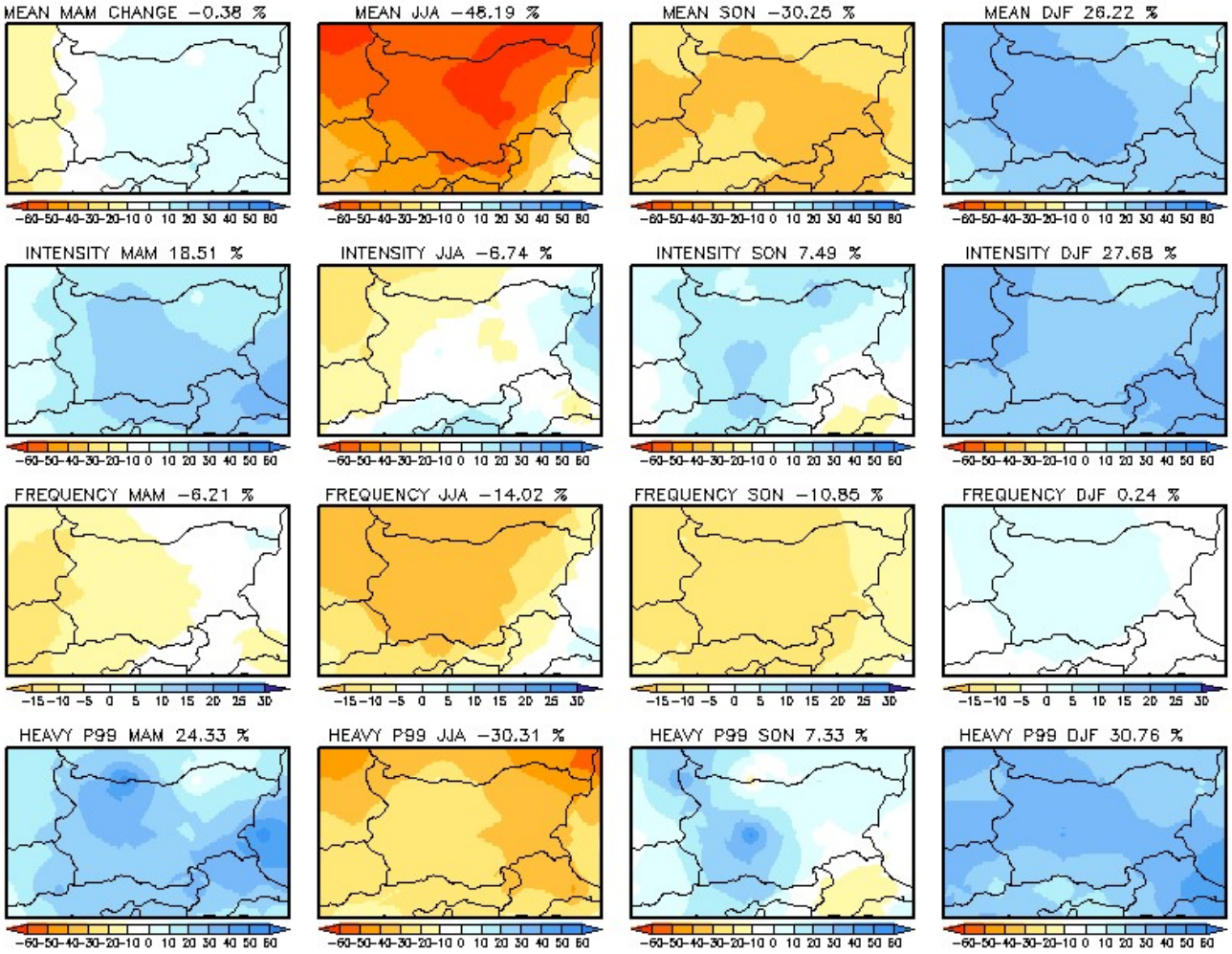

Figure S10. Expected changes in mean daily precipitation (first row), precipitation intensity (second row), frequency (third row), and heavy rainfall (p99) (last row) from driving GCM HadGEM2-ES according to the RCP8.5 scenario related to the spring—MAM (first column), summer—JJA (second columns), fall—SON (third column), and winter—DJF (last column) projected at the end of the century (2089–2098) concerning the historical period (1995–2004) in %.